5-1-2018

Inhibition of Aldehyde Dehydrogenase-Activity Expands Multipotent Myeloid Progenitor Cells with Vascular Regenerative Function

Tyler T. Cooper
Western University

Stephen E. Sherman
Western University

Miljan Kuljanin
Western University

Gillian I. Bell
Robarts Research Institute

Gilles A. Lajoie
Western University

See next page for additional authors

STEM CELLS®

REGENERATIVE MEDICINE

Inhibition of Aldehyde Dehydrogenase-Activity Expands Multipotent Myeloid Progenitor Cells with Vascular Regenerative Function

TYLER T. COOPER,[a,b] STEPHEN E. SHERMAN,[a,b] MILJAN KULJANIN,[b,c] GILLIAN I. BELL,[b] GILLES A. LAJOIE,[c] DAVID A. HESS [a,b]

Key Words. Aldehyde dehydrogenase • Transplantation • Hematopoietic stem cells • Proteomics

[a]Department of Physiology and Pharmacology, and [c]Don Rix Protein Identification Facility, Department of Biochemistry, Western University, London, Ontario, Canada; [b]Molecular Medicine Research Laboratories, Krembil Centre for Stem Cell Biology, Robarts Research Institute, London, Ontario, Canada

Correspondence: David A. Hess, Ph.D., Department of Physiology and Pharmacology, Schulich School of Medicine and Dentistry, Western University, 1151 Richmond Street, London, Ontario, Canada N6A 5B7. Telephone: 519-931-5777, ext. 24152; e-mail: dhess@robarts.ca

Received September 26, 2017; accepted for publication January 12, 2018; first published online in STEM CELLS *EXPRESS* January 27, 2018.

http://dx.doi.org/10.1002/stem.2790

ABSTRACT

Blood-derived progenitor cell transplantation holds potential for the treatment of severe vascular diseases. Human umbilical cord blood (UCB)-derived hematopoietic progenitor cells purified using high aldehyde dehydrogenase ($ALDH^{hi}$) activity demonstrate pro-angiogenic functions following intramuscular (i.m.) transplantation into immunodeficient mice with hind-limb ischemia. Unfortunately, UCB $ALDH^{hi}$ cells are rare and prolonged ex vivo expansion leads to loss of high ALDH-activity and diminished vascular regenerative function. ALDH-activity generates retinoic acid, a potent driver of hematopoietic differentiation, creating a paradoxical challenge to expand UCB $ALDH^{hi}$ cells while limiting differentiation and retaining pro-angiogenic functions. We investigated whether inhibition of ALDH-activity during ex vivo expansion of UCB $ALDH^{hi}$ cells would prevent differentiation and expand progeny that retained pro-angiogenic functions after transplantation into non-obese diabetic/severe combined immunodeficient mice with femoral artery ligation-induced unilateral hind-limb ischemia. Human UCB $ALDH^{hi}$ cells were cultured under serum-free conditions for 9 days, with or without the reversible ALDH-inhibitor, diethylaminobenzaldehyde (DEAB). Although total cell numbers were increased >70-fold, the frequency of cells that retained $ALDH^{hi}$/CD34+ phenotype was significantly diminished under basal conditions. In contrast, DEAB-inhibition increased total $ALDH^{hi}$/CD34+ cell number by $\geq$10-fold, reduced differentiation marker (CD38) expression, and enhanced the retention of multipotent colony-forming cells in vitro. Proteomic analysis revealed that DEAB-treated cells upregulated anti-apoptotic protein expression and diminished production of proteins implicated with megakaryocyte differentiation. The i.m. transplantation of DEAB-treated cells into mice with hind-limb ischemia stimulated endothelial cell proliferation and augmented recovery of hind-limb perfusion. DEAB-inhibition of ALDH-activity delayed hematopoietic differentiation and expanded multipotent myeloid cells that accelerated vascular regeneration following i.m. transplantation in vivo. STEM CELLS *2018;36:723–736*

SIGNIFICANCE STATEMENT

This article demonstrates a novel method to generate clinically applicable numbers of human umbilical cord blood-derived myeloid progenitor cells with high aldehyde dehydrogenase ($ALDH^{hi}$)-activity by limiting retinoic acid-induced differentiation ex vivo. Furthermore, ALDH inhibition prevented megakaryocyte maturation, expanded myeloid multipotent progenitor cells possessed a pro-angiogenic and pro-survival proteome and exhibited vascular regenerative function after intramuscular transplantation into non-obese diabetic/severe combined immunodeficient mice with femoral artery ligation-induced hind limb ischemia.

INTRODUCTION

Systemic atherosclerosis results in impaired blood vessel architecture and function [1], leading to peripheral arterial disease (PAD) characterized by obstructed blood flow within the peripheral vasculature, limiting delivery of oxygen and nutrients to afflicted tissues [2]. Clinical presentation of PAD ranges from asymptomatic ischemia to exercise-induced intermittent claudication, which may progress toward critical limb ischemia (CLI), the most severe manifestation of PAD. Patients with CLI suffer from pain at rest, non-healing tissue ulceration, and life-threatening infections. Current pharmaceutical therapies target risk factors to reduce cardiovascular events, whereas endovascular or surgical bypass interventions

aim to recover perfusion to afflicted tissues. Unfortunately, these therapies provide only short-term benefit and are not offered to individuals with diffuse CLI [3–6]. As a result, 25%–30% of CLI patients require limb amputation within the first year of diagnosis [7], and >60% of CLI patients will succumb to death within 5 years [8]. There is a need to develop effective therapies for the 8–12 million North Americans and >200 million individuals worldwide afflicted with advancing PAD [7].

Tissue revascularization via "therapeutic angiogenesis" has been proposed as a potential target for combating severe PAD. Robust angiogenesis can occur in skeletal muscle following ischemic injury; however, this requires activation of several cell types to orchestrate vascular remodeling or to activate flow within collateral vessels [9, 10]. Pro-angiogenic cytokine/chemokine secretion by hematopoietic progenitor cells (HPCs) direct sprouting by vessel-forming endothelial progenitor cells (EPC) and encourage infiltration by vessel wrapping pericytes, respectively; two processes essential for stable neovessel formation [10]. Thus, cellular therapies to induce revascularization uses the secretory properties of transplanted blood-derived progenitor cells to generate a pro-angiogenic microenvironment and restore revascularization within ischemic tissues [11].

We have previously demonstrated the vascular regenerative potential of HPC isolated from healthy human bone marrow (BM) and umbilical cord blood (UCB) [12, 13]. Notably, purification of cells with high aldehyde dehydrogenase (ALDH) activity ($ALDH^{hi}$), a detoxification function conserved in progenitor cells of multiple lineages, promoted revascularization following transplantation into mice with hind-limb ischemia, by stimulating endogenous capillary formation at the site of injury without permanent incorporation into regenerating murine neovessels [13]. Moreover, $ALDH^{hi}$ cells from BM or UCB are also enriched for rare non-HPCs (EPC and multipotent stromal cells), with a larger representation of myeloid HPC [12–15]. In 2011, a randomized Phase I clinical trial by Perin et al. demonstrated that intramuscular (i.m.) transplantation of autologous BM $ALDH^{hi}$ cells significantly improved Rutherford's Category scores and ankle-brachial index measurements from baseline in patients with non-operational CLI, but did not improve ischemic ulcer healing [16]. These results provided rationale for a Phase II trial (PACE trial) which aimed to stimulate revascularization in patients with intermittent claudication, thereby mitigating progression toward end-stage CLI [17]. This double-blinded multicenter study recently reported that transplantation of autologous BM-derived $ALDH^{hi}$ cells was unable to effectively improve exercise performance or blood perfusion via collateral vessel formation after 6 months [18].

Although the preclinical data used to initiate early clinical studies were promising [13], several factors may explain why the preclinical efficacy in murine models does not accurately predict clinical efficacy in humans. The preclinical experiments were performed using healthy human BM $ALDH^{hi}$ cells transplanted into immunodeficient mice with surgically induced limb ischemia. Femoral artery ligation (FAL) in mice has been the gold-standard preclinical model to assess therapeutic angiogenesis elicited by pharmaceuticals or cells; however, the model does possess several limitations which need to be addressed to improve clinical translation. Specifically, this model mimics an acute ischemic injury occurring in young and healthy animals, and does not reflect the chronic ischemic microenvironment occurring in human patients due to the buildup of atherosclerotic plaques over an extended period of time. In addition to physiological differences between species (i.e., heart rate and plasma cholesterol), patients with PAD commonly demonstrate other influential factors, chronic inflammation, smoking, and sedentary lifestyles, which are difficult to mimic in a murine model. Furthermore, emerging preclinical evidence also indicates autologous BM mononuclear cells (MNC) harvested from patients with chronic atherosclerosis and associated comorbidities exhibit severe functional impairments [19, 20]. Endothelial cells derived from healthy animals exhibited vascular regenerative functions in a diabetic model of myocardium ischemia, whereas, cells harvested from diabetic animals failed to induce vasculogenesis [21]. Several studies have aimed to increase clinical efficacy by purification of select subpopulations (CD34+) derived from autologous BM-MNC [22]; however, this approach has provided a modest benefit over transplantation of unpurified BM-MNC. Alternatively, using healthy allogenic sources may improve the efficacy of cell-based therapies, by limiting the exposure of therapeutic cells to the damaging microenvironment of chronic disease [23, 24].

ALDH provides protection to long-lived stem and progenitor cell populations from cytotoxic insults [25]. Representing a conserved stem cell function and coinciding with primitive surface marker expression (CD34+), $ALDH^{hi}$-activity rapidly diminishes as multipotent HPC differentiate toward more expendable lineage-restricted phenotypes [15]. ALDH also represents the rate-limiting enzyme in the production of retinoic acid (RA), a potent driver of hematopoietic differentiation. RA activates the retinoic acid receptor (RAR) - retinoid X receptor (RXR) nuclear receptor complex that regulates mRNA transcription and epigenetic modifications [26], resulting in hematopoietic cell differentiation. For example, activation of RAR/RXR induces the expression cyclic-ribose ADP hydrolase (CD38), a membrane-bound enzyme implicated with hematopoietic cell differentiation [27]. Therefore, the ex vivo expansion of UCB $ALDH^{hi}$ cells represents a paradoxical challenge to increase primitive and pro-angiogenic $ALDH^{hi}$ cell numbers while limiting RA-induced hematopoietic differentiation.

We have recently shown that UCB $ALDH^{hi}$ cells can be efficiently expanded under serum-free conditions to generate hematopoietic progeny retaining vascular regenerative functions in vivo [28]. However, as culture time was increased from 6 to 9 days, expanded progeny failed to retain vascular regenerative functions. In addition, reducing RA-production by inhibition of ALDH-activity during ex vivo expansion augmented the number of CD34+ HPC with *SCID*-repopulation capacity [29, 30]. Therefore, we sought to determine whether inhibition of ALDH-activity, using diethylaminobenzaldehyde (DEAB) treatment, would enhance the expansion of UCB $ALDH^{hi}$ cells without loss of vascular regenerative functions assessed after i.m. transplantation into mice with FAL-induced unilateral hind-limb ischemia.

Materials and Methods

Detailed Methods have been provided in Supporting Information Materials that describe routine, previously published

procedures in our laboratory such as UCB ALDH^{hi} cell isolation [12], flow cytometric characterization of cell surface phenotype [15], and hematopoietic progenitor colony formation [28]. Also included in Supporting Information Methods is detailed descriptions of transplantation experiments performed with immunodeficient mice after FAL surgery [12], analyses of limb perfusion using laser Doppler perfusion imaging [12], gait analyses by Catwalk imaging [28], and immunohistochemical analyses used to characterize vessel regeneration and human cell engraftment in ischemic muscle [28]. Novel culture conditions and proteomic analyses unique to this article are described below.

Expansion of UCB ALDH^{hi} Cells in Culture

UCB ALDH^{hi} cells were plated on fibronectin-coated flasks and expanded in serum-free X-vivo 15 (Lonza, Basel, Switzerland) supplemented with 10 ng/ml thrombopoietin (TPO), Fms-like tyrosine kinase 3 ligand (FLT-3L), and stem cell factor (SCF) for up to 9 days, herein referred to as Basal conditions. All growth factors were purchased from Life Technologies (Carlsbad, CA). To inhibit ALDH-activity and limit cell differentiation, 1.0×10^{-5} mol/l diethylaminobenzaldehyde (DEAB) (Stem Cell Technologies, Vancouver, Canada) was added to Basal conditions between days 3 and 6 of ex vivo expansion, herein referred to as DEAB-treated conditions. DEAB dose and treatment kinetics were optimized based on maximal retention of ALDH^{hi} cells at endpoint. Complete media change was performed every 3 days.

Generation of HPC-Conditioned Media and Cell Lysates for Proteomic Analyses

Expanded cells were harvested and washed with phosphate-buffered saline (PBS) to remove residual growth factors and resuspended in fresh RPMI 1640 + 10 ng/ml of SCF, TPO, and FLT-3L for 24 hours to generate conditioned media (CdM) in biological triplicate. CdM was centrifuged to remove cellular debris and concentrated using 3 kDa molecular weight cutoff filter units (Millipore, Bedford, MA). Concentrated CdM was lyophilized overnight and resuspended in 8 mol/l urea, 5.0×10^{-2} mol/l ammonium bicarbonate, 1.0×10^{-2} mol/l dithiothreitol, and 2% SDS solution before secreted protein quantitation and fractionation. Expanded cell pellets were lysed in 8 M urea buffer, and sonicated (20 × 0.5 second pulses; level 1) to shear DNA. Protein concentrations were estimated using the Pierce 660 nm protein assay (ThermoFisher Scientific, Waltham, MA).

Chloroform/Methanol Precipitation and Protein Digestion

Cell lysates or CdM were reduced in 1.0×10^{-2} mol/l dithiothreitol for 30 minutes and alkylated in 1.0×10^{-1} mol/l iodoacetamide for 30 minutes. Samples were precipitated in chloroform/methanol in 1.5 ml microfuge tubes [31]; 50 μg aliquots of each sample were topped up to 150 μl with 5.0×10^{-2} mol/l ammonium bicarbonate, 600 μl of ice cold methanol, followed by 150 μl of chloroform; 450 μl of water was added before vortexing and centrifugation at 14,000*g* for 5 minutes. The upper/aqueous methanol phase was removed and 450 μl of ice cold methanol was added before vortexing and centrifugation. Precipitated protein pellet was air dried before protein digestion. For on-pellet protein digestion, 100 μl of 5.0×10^{-2} mol/l ammonium bicarbonate (pH 8.0) trypsin/LysC (1:50 ratio, enzyme:sample) (Promega, Madison, WI) solution was added before incubation overnight at 37°C in water bath shaker. Trypsin (1:100 ratio) was added for 4 hours before acidifying with 10% formic acid (pH 3–4). Digests were centrifuged at 16,000*g* to remove insoluble material. Peptide concentrations were estimated using a BCA assay (ThermoFisher Scientific).

SCX Peptide Fractionation

Tryptic peptides recovered from chloroform/methanol precipitation of cell lysates or CDM (50 μg) were fractionated using SCX StageTips [32]. Peptides were acidified using 1% Trifluoroacetic acid and loaded onto a 12-plug StageTips. Six SCX fractions were collected by eluting in 7.5×10^{-2}, 1.25×10^{-1}, 2.0×10^{-1}, 2.50×10^{-1}, and 3.0×10^{-1} mol/l ammonium acetate/20% acetonitrile/0.5% formic acid (FA) solutions followed by elution with 5% (w/v) ammonium hydroxide/80% ACN. Fractions were dried in a SpeedVac, resuspended in double distilled water and dried again to remove residual ammonium acetate. All samples were resuspended in 0.1% FA before liquid chromatography–tandem mass spectrometry (LC-MS)/MS analysis.

Liquid Chromatography–Tandem Mass Spectrometry

One microgram of sample was injected into a Waters nanoAcquity HPLC system (Waters, Milford, MA) coupled to an ESI Orbitrap mass spectrometer (Orbitrap Elite or QExactive, ThermoFisher Scientific). Buffer A consisted of water/0.1% FA and buffer B consisted of ACN/0.1% FA. All samples were trapped for 5 minutes at a flow rate of 10 μl/minute using 99% Buffer A, 1% Buffer B on a Symmetry BEH C18 Trapping Column, 5 μm, 180 μm × 20 mm (Waters). Peptides were separated using a Peptide BEH C18 Column, 130Å, 1.7 μm, 75 μm × 250 mm operating at a flow rate of 300 nl/minute at 35°C (Waters). Cell lysate samples were separated using a nonlinear gradient consisting of 5%–7.5% B over 1 minute, 7.5%–25% B over 180 minutes and 25%–60% B over 240 minutes before increasing to 98% B and washing. CdM samples were separated using a nonlinear gradient consisting of 1%–7% B over 3.5 minutes, 7%–19% B over 90 minutes, and 19%–30% B over 120 minutes before increasing to 95% B and washing. Settings for data acquisition on the Orbitrap Elite and QExactive are provided in Supporting Information Table S6.

Proteomic Data Analyses

Data analysis was performed using PEAKS 8.0 software (Bioinformatics Solutions Inc., Waterloo, ON, Canada). Raw data files were refined using correct precursor mass and de novo sequencing was performed using the following parameters: parent mass tolerance 20 ppm; fragment ion tolerance 0.80 Da; enzyme was set to trypsin. Data analyses were searched against the Uniprot human sequence database (20,178 entries). Quantitative data analysis was performed using MaxQuant version 1.5.2.8 [33]. Protein and peptide false discovery rate were set to 0.01 (1%), while the decoy database was set to revert. All parent and fragment tolerances were set as described above. The match between runs was enabled and all other parameters left at default. Data were analyzed using label free quantitation and intensity-based absolute

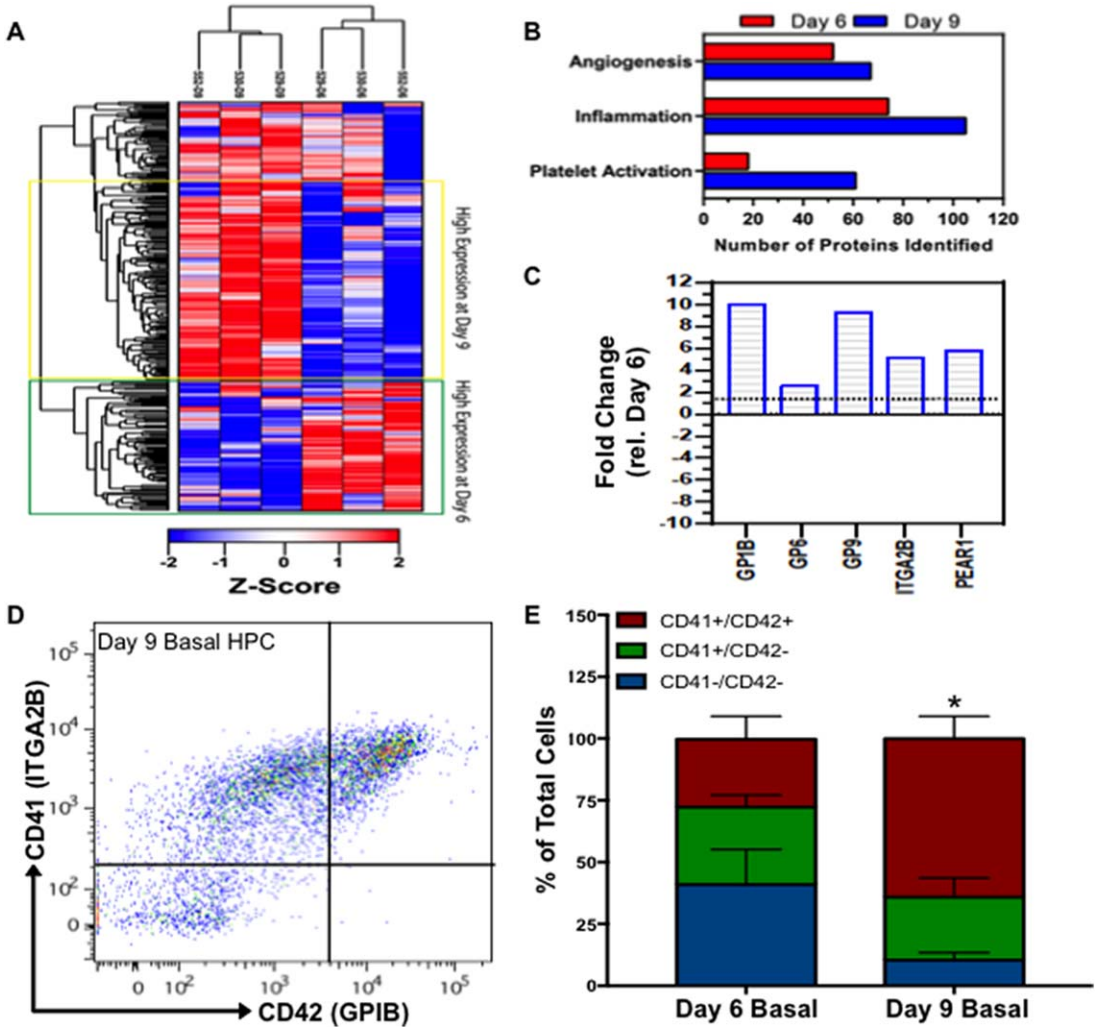

Figure 1. Umbilical cord blood ALDH^{hi} cells differentiated toward a megakaryocyte phenotype when cultured under Basal conditions. Viable day 6 ($N = 3$) or day 9 ($N = 3$) cells expanded under Basal conditions were replated in RPMI 1640 + stem cell factor, thrombopoietin, Fms-like tyrosine kinase 3 ligand for 24 hours to generate conditioned media (CdM). **(A):** Mass spectrometry analyses of CdM revealed distinct secretome profiles. **(B):** The secretory profile of day 9 cells was highly enriched with proteins implicated in platelet activation. **(C):** day 9 cells significantly upregulated the expression of CD41 (ITGA2B) and CD42 (GPIB), compared with day 6 cells. **(D, E):** Increased culture time under Basal conditions enriched for cells with a megakaryocyte cell surface phenotype (CD41+/CD42+). Data represented as mean ± SEM (*, $p < .05$; $N = 5–7$). Statistical analyses were determined by paired Student's *t* test. Abbreviations: GPIB, CD41 (ITGA2B) and CD42; HPC, hematopoietic progenitor cell.

quantification as described previously [34]. Bioinformatic analysis was performed using Perseus version 1.5.0.8 and proteins identified by site, reverse and contaminants were removed manually. When using the match between runs feature, datasets were filtered for proteins containing a minimum of one unique peptide in at least two biological replicates. Missing values were replaced using data imputation by using a width of 0.3 and a downshift of 1.2 [35].

Statistical Analyses

A multiple sample *t* test was performed in Perseus comparing the cell lysates for day 9 Basal versus DEAB for proteomic analysis; and day 6 Basal versus day 9 Basal for secretome analysis. Statistical analysis for flow cytometry, quantitative polymerase chain reaction (qPCR), hematopoietic colony forming-cell analyses was performed using a student's *t* test within each time point. Analysis of significance was performed by one-way analysis of variance with Tukey's multiple comparisons tests for all in vivo experiments and enumeration of myeloid-specific colony formation. Outliers were identified using Grubb's test; $p < .05$.

Results

Basal Conditions Promoted Expansion of Cells with Megakaryocyte Secretory Profile

We have recently demonstrated UCB ALDH^{hi} cells expanded under Basal conditions for 6 but not 9 days, accelerated the recovery of hindlimb perfusion after transplantation [28]. This led us to investigate whether additional culture time (3 days) changed the secretory profile of expanded hematopoietic

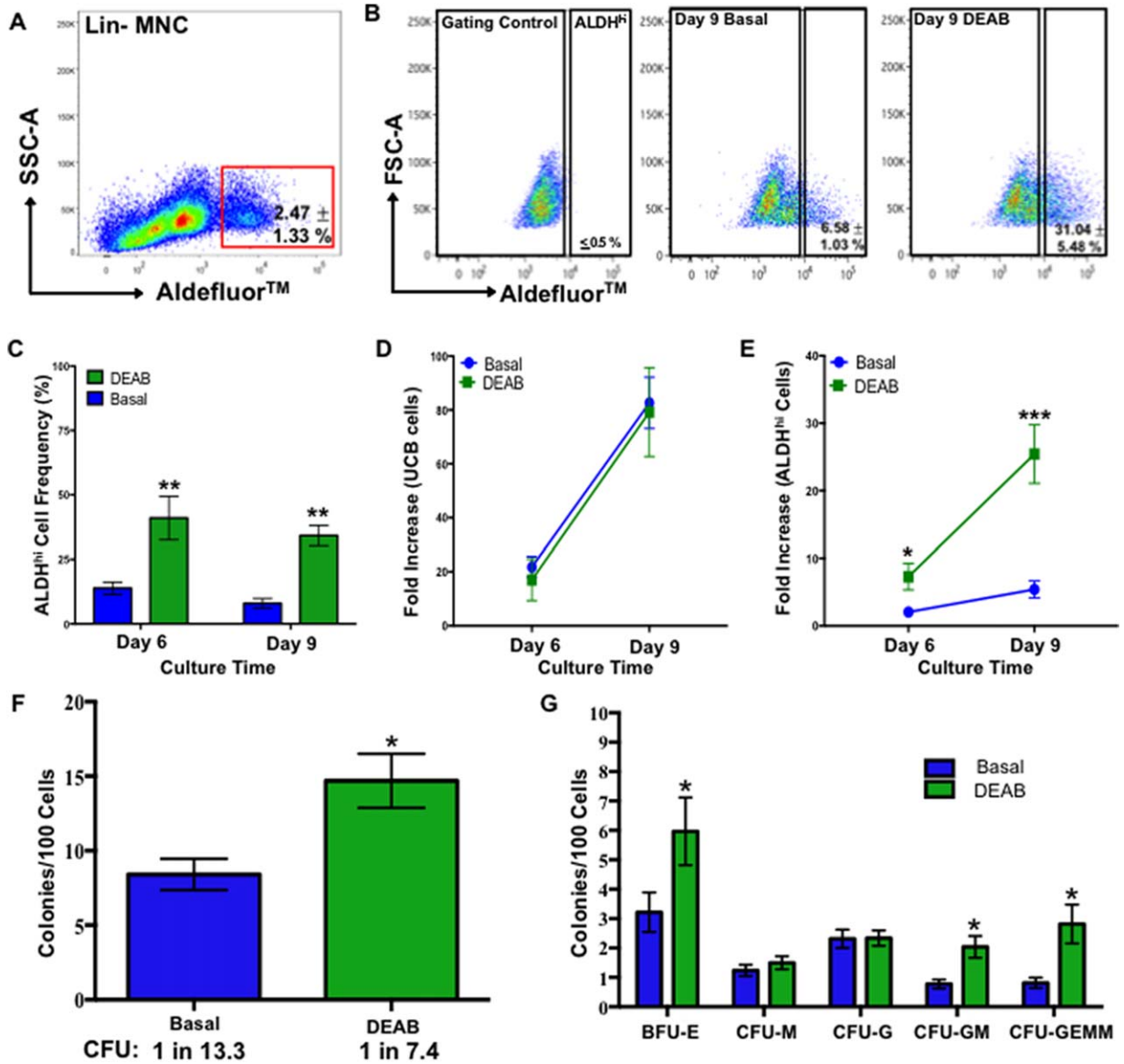

Figure 2. Diethylaminobenzaldehyde (DEAB)-treatment augmented the expansion of early myeloid progenitors with high ALDH-activity. **(A):** Umbilical cord blood ALDH^{hi} cells were isolated by fluorescence-activated cell sorting and expanded with or without DEAB-treatment between days 3 and 6. **(B):** Representative flow cytometry plots showing DEAB-treatment enhanced **(C)** the frequency of ALDH^{hi} cells retained after 9 days ($N = 7$). **(D):** Total cell expansion was not affected by DEAB-treatment, whereas **(E):** total ALDH^{hi} cell number was increased ~25-fold under DEAB-treated conditions. **(F):** DEAB-treatment increased the hematopoietic colony forming capacity of expanded cells seeded in methylcellulose media ($N = 5$). **(G):** DEAB-treatment enhanced the production of colonies with multiple myeloid phenotypes. Data represented as mean ± SEM (*, $p < .05$; **, $p < .01$; ***, $p < .001$). Statistical analyses were determined by paired Student's *t* test. Abbreviations: BFU-E, burst forming unit-erythrocyte; CFU, colony forming unit; DEAB, diethylaminobenzaldehyde; FSC, forward scatter; MNC, mononuclear cells; SSC, side scatter; UCB, umbilical cord blood.

progeny, thereby limiting vascular regenerative function in vivo. Mass spectrometry proteomic analysis was used to determine changes in the secretome of cells harvested after culture under Basal conditions ($N = 3$) at day 6 or day 9. A total of 5,404 unique proteins were detected, with 3,636 proteins identified in CdM generated by both day 6 and day 9 expanded cells; 325 proteins or 1443 proteins were exclusively contained within CdM generated from day 6 or day 9 cells, respectively. Major cytokines associated with angiogenesis were present in CdM generated from both expanded cell populations. Therefore, we focused on the relative quantity of proteins commonly secreted. Of the 3,636 common proteins secreted, 144 and 317 proteins were significantly increased in day 6 and day 9 CdM, respectively. Distinct patterns of expression were identified reflecting widespread changes in protein expression as culture time was increased (Fig. 1A). Although day 6 and day 9 cells demonstrated polarized regenerative function in vivo [23], the secretion of proangiogenic proteins, such as vascular endothelial growth factor (VEGF)-A and angiopoietin 1 (ANGPT1), was comparable between expanded cell populations. Interestingly, proteins involved in inflammation and platelet activation were enriched within CdM generated from day 9 cells (Fig. 1B). For example, platelet activation-associated proteins significantly increased in

Table 1. DEAB-treatment enhanced the expansion of cells with a primitive surface phenotype

Expanded HPC		% of Total cells			
Population	Phenotype	Day 6 Basal	Day 6 DEAB	Day 9 Basal	Day 9 DEAB
BULK	CD34+	20.71 ± 2.09	22.20 ± 2.51	9.49 ± 1.03	9.37 ± 1.53
	CO34+ CD38–	11.77 ± 2.14	**17.19 ± 2.09***	7.43 ± 1.05	7.57 ± 1.21
	CD38+	20.24 ± 5.77	**11.09 ± 2.36***	31.06 ± 2.52	**21.16 ± 2.56****
$ALDH^{hi}$	CD34+	5.72 ± 1.36	**11.46 ± 1.77***	2.18 ± 0.42	**6.20 ± 0.73***
	CD34+ CD38–	2.77 ± 0.70	**9.20 ± 1.36***	2.29 ± 0.35	**5.46 ± 0.59*****
	CD38+	6.22 ± 1.95	5.31 ± 0.90	2.95 ± 0.84	**8.94 ± 1.73***
$ALDH^{lo}$	CD34+	**10.98 ± 1.32***	6.34 ± 1.48	5.64 ± 0.80	**2.47 ± 0.76*****
	CD34+ CD38–	7.01 ± 1.17	5.56 ± 1.36	3.96 ± 0.69	**1.75 ± 0.58***
	CD38+	6.62 ± 2.60	3.78 ± 1.04	24.59 ± 181	**6.25 ± 2.70*****

Statistical analyses were determined by Student's *t* test compared within each time point.
Data expressed as mean ± SEM (*$p < 0.05$, **$p < 0.01$, ***$p < 0.001$: $N = 5$–9).

CdM generated from day 9 cells included integrin alpha-IIb (ITGA2B, CD41), glycoprotein Ib (GP1B, CD42), glycoprotein IX (GP9), and platelet endothelial aggregation receptor 1 (Fig. 1C). Flow cytometry was used to validate expression of CD41 and CD42, classic markers of megakaryocyte-lineage differentiation (Fig. 1D). These analyses demonstrated that expansion of UCB-derived $ALDH^{hi}$ cells under Basal conditions enriched for cells with a committed megakaryocyte ($CD41^{+}$/$CD42^{+}$) phenotype as culture time progressed from 6 to 9 days (25.76 ± 5.14% vs. 54.7 ± 6.50%; *, $p < .05$; Fig. 1E). Importantly, this end-stage megakaryocyte differentiation was also associated with the loss of vascular regenerative capacity after transplantation [28].

DEAB-Treatment Augmented $ALDH^{hi}$ Cell Expansion

$ALDH^{hi}$ cells represented only 2.47 ± 1.33% Lin^{-} cells (Fig. 2A) correlating to ≤0.5% of total MNC collected. In addition, UCB $ALDH^{hi}$ cells rapidly reduce ALDH-activity (Fig. 2B) during ex vivo expansion [28]. Therefore, $ALDH^{hi}$ cells were expanded with or without DEAB-treatment, to inhibit ALDH-activity and limit RA-induced differentiation during culture (Fig. 2B). Exposure of cells to DEAB-treatment at days 3–6 was selected based on the optimal preservation of $ALDH^{hi}$ cells during 6 and 9 days expansion ex vivo (Supporting Information Fig. S1). Temporal DEAB-treatment from days 3 to 6 increased expanded $ALDH^{hi}$ cell frequency at day 6 (40.98 ± 8.43% vs. 13.85 ± 2.38%; **, $p < .01$) and at day 9 (31.04 ± 5.48% vs. 6.58 ± 1.03%; **, $p < .01$; Fig. 2C). Total cell expansion kinetics were equivalent over 9 days with or without DEAB-treatment (82.62 ± 9.51-fold vs. 79.22 ±16.49-fold increase; Fig. 2D.). Taken together, DEAB-treatment led to a 25.42 ± 4.35-fold increase in $ALDH^{hi}$ cell numbers obtained after 9 days; a significant increase compared with Basal conditions (5.40 ± 1.27-fold increase; ***, $p < .001$; Fig. 2E). Therefore, DEAB-treatment from days 3 to 6 during a 9-day expansion protocol was selected for further assessment of primitive progenitor cell phenotype and function.

RA-Signaling Was Modified following DEAB-Treatment

ALDH-activity leads to the production of RA, a potent driver of hematopoietic differentiation. To validate that DEAB-treatment modulated RA-signaling during expansion, we first performed reverse transcriptase-qPCR on transcriptional targets of the RAR/RXR complex. Activation of the RAR/RXR complex was expected to increase transcription of target genes such as *CYP26A1*, *ALDH1A3* isoform, and *RAR* [25]. DEAB-treatment significantly reduced transcription of ALDH1A3, CYP26A1, and RARα subunit while transcription of RARγ was increased (Supporting Information Fig. S2). Collectively, this suggested RA-signaling networks were modified following DEAB-treatment.

DEAB-Treatment Enriched for Cells with Multipotent Myeloid Progenitor Function

To determine whether expanded cells retained hematopoietic colony forming unit (CFU) functions in vitro, day 9 cultured cells were seeded in methylcellulose media and enumerated for myeloid-lineage colony formation after 14 days. DEAB-treated cells demonstrated a significantly higher frequency (*, $p < .05$) of total colony formation (1 CFU in 7.4 cells) compared with cells expanded under Basal conditions (1 CFU in 13.3 cells; Fig. 2F). DEAB-treatment enriched specifically for early HPC with myeloid multipotentcy; enumerated by colonies demonstrating multiple myeloid morphologies (Fig. 2G). Thus, DEAB treatment augmented the expansion of $ALDH^{hi}$ cells that retained multipotent hematopoietic CFU capacity in vitro.

DEAB-Treatment Enriched for Cells with Primitive Surface Marker Expression

To determine whether DEAB-treatment also prevented the loss of primitive cell surface phenotype ($ALDH^{hi}$/$CD34^{+}$/$CD38^{-}$) during expansion, cells were analyzed using multicolor flow cytometry (Table 1). At day 9, expanded cells were exclusively hematopoietic determined by pan-leukocyte marker (CD45) expression (>99%), and the majority of Basal or DEAB-treated cells expressed the early myeloid cell surface marker CD33 (96.1 ± 0.85 and 94.5 ± 1.53%, Supporting Information Table S1). Monocyte-specific marker (CD14) expression was comparable between Basal and DEAB-treated conditions (2.96 ± 1.23 vs. 4.08 ± 1.64% of total cells). compared with Basal conditions, expression of the hematopoietic differentiation marker CD38 was significantly reduced following DEAB-treatment (31.06 ± 2.52 vs. 21.16 ± 2.56% of total cells; **, $p < .01$; Table 1). Futhermore, DEAB-treatment enriched for cells with primitive $ALDH^{hi}$/CD34+ (2.18 ± 0.42 vs. 6.20 ± 0.73% of total cells; *, $p < .05$) and $ALDH^{hi}$/CD34+/$CD38^{-}$ (2.29 ± 0.35 vs. 5.46 ± 0.59% of total cells; ***, $p < .001$) phenotypes (Table 1). Collectively, DEAB-treatment generated 5- and 10-fold increase in the total number of $ALDH^{hi}$ CD34+ or $ALDH^{hi}$ CD34+/$CD38^{-}$ after 9 days, respectively (Supporting

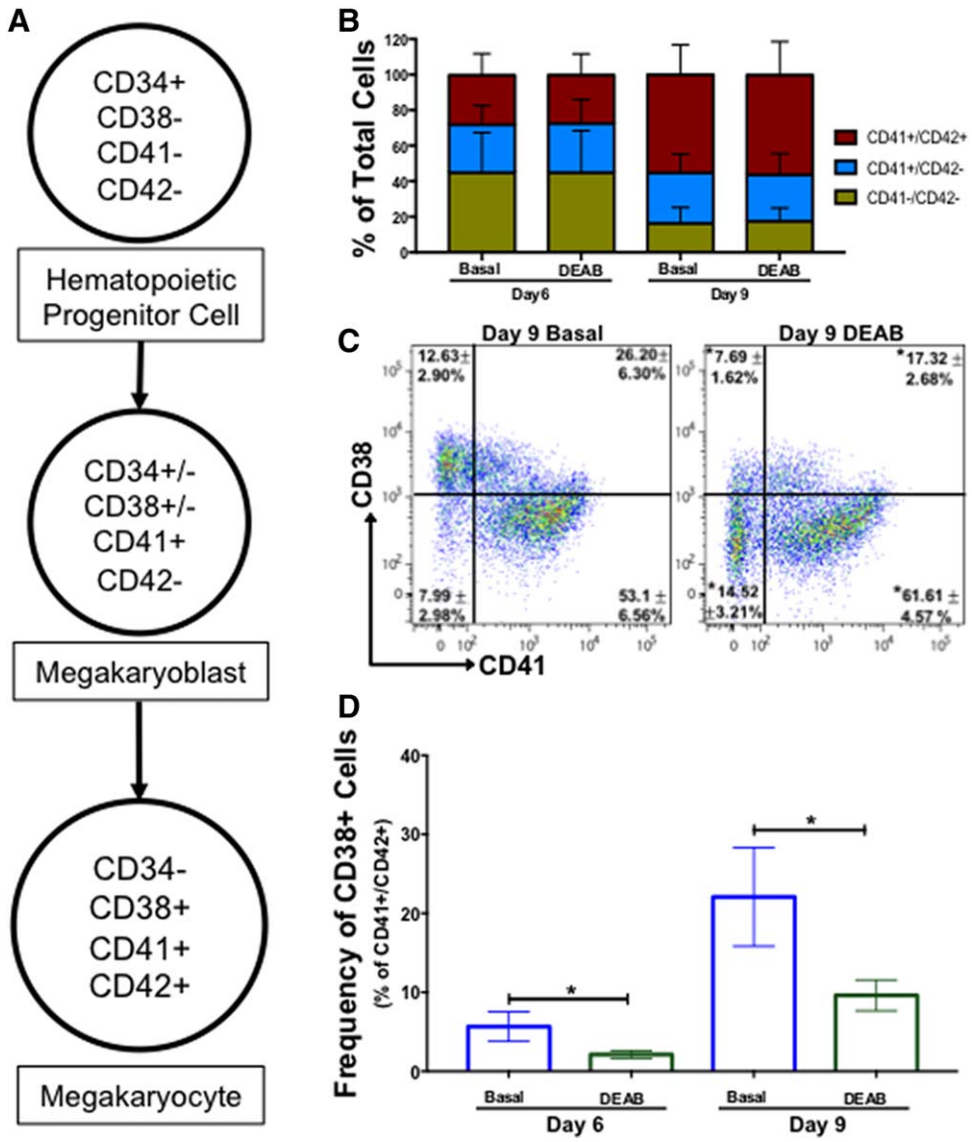

Figure 3. Diethylaminobenzaldehyde (DEAB)-treatment reduced differentiation toward megakaryocyte phenotype. **(A):** Schematic representation of megakaryopoiesis and acquisition of mature megakaryocyte phenotype (CD41/CD42+/CD38+). **(B):** DEAB-treatment did not alter CD41 and CD42 expression patterns at 6 or 9 days. **(C):** Representative flow cytometry plots showing reduced expression of CD38 on $CD41^{+/-}$ cells generated under DEAB-treated conditions. **(D):** CD38 expression was reduced on megakaryocytes ($CD41^{+}/CD42^{+}$) under DEAB-treated conditions. Data represented as mean ± SEM (*, $p < .05$; $N = 5–8$). Statistical analyses were performed by paired Student's *t* test. Abbreviation: DEAB, diethylaminobenzaldehyde.

Information Table S2). In contrast, Basal conditions generated a modest 1.7- and 4.1-fold increase in the number of $ALDH^{hi}$ CD34+ or $ALDH^{hi}$ CD34+/$CD38^{-}$, respectively. Basal conditions highly enriched for cells with mature hematopoietic cell ($ALDH^{lo}/CD38^{+}$) phenotype (24.59 ± 1.81 vs. 6.25 ± 2.70% of total cells; ***, $p < .001$; Table 1). Collectively, DEAB-treatment enhanced the expansion of hematopoietic cells retaining $ALDH^{hi}$-activity and primitive cell surface marker expression patterns.

DEAB-Treatment Reduced Megakaryocyte Lineage Maturation

Basal culture conditions led to UCB $ALDH^{hi}$ cell differentiation toward a megakaryocyte phenotype as culture time progressed (Fig. 1). Therefore, we sought to determine whether DEAB-treatment delayed differentiation of expanded $ALDH^{hi}$ cells toward the megakaryocyte lineage (Fig. 3A). Although we did not observe differences in the frequency of expanded cells acquiring mature megakaryocyte phenotype ($CD41^{+}/CD42^{+}$) at day 9 (Fig. 3B), DEAB-treatment significantly reduced the frequency of $CD41^{+}$ cells that coexpressed CD38 (17.3 ±2.7 vs. 26.2 ± 6.4% of CD41+ cells; Fig. 3C; *, $p < .05$, and Supporting Information Table S3). Furthermore, DEAB-treatment significantly reduced the expression of CD38 on $CD41^{+}/CD42^{+}$ megakaryocytes, compared with Basal conditions (*, $p < .05$; Fig. 3D). Previous reports have also suggested that expanded $CD41^{+}/CD42^{-}$ hematopoietic cells retain myeloid multipotentcy in vitro and *SCID*-repopulating capacities in vivo when coexpressing a $CD34^{+}/CD38^{-}$ phenotype [36]. At day 9, DEAB-treatment enriched the $CD41^{+}/CD42^{-}$ megakaryoblast fraction with primitive CD34+/$CD38^{-}$ phenotype (13.1 ± 2.4% vs. 8.2 ± 2.0%; *, $p < .05$; Supporting Information Table

S3). Collectively, these results suggested that DEAB-treatment delayed the maturation of CD41+/CD42$^-$ megkaryoblasts by delaying CD38 acquisition and loss of CD34 expression.

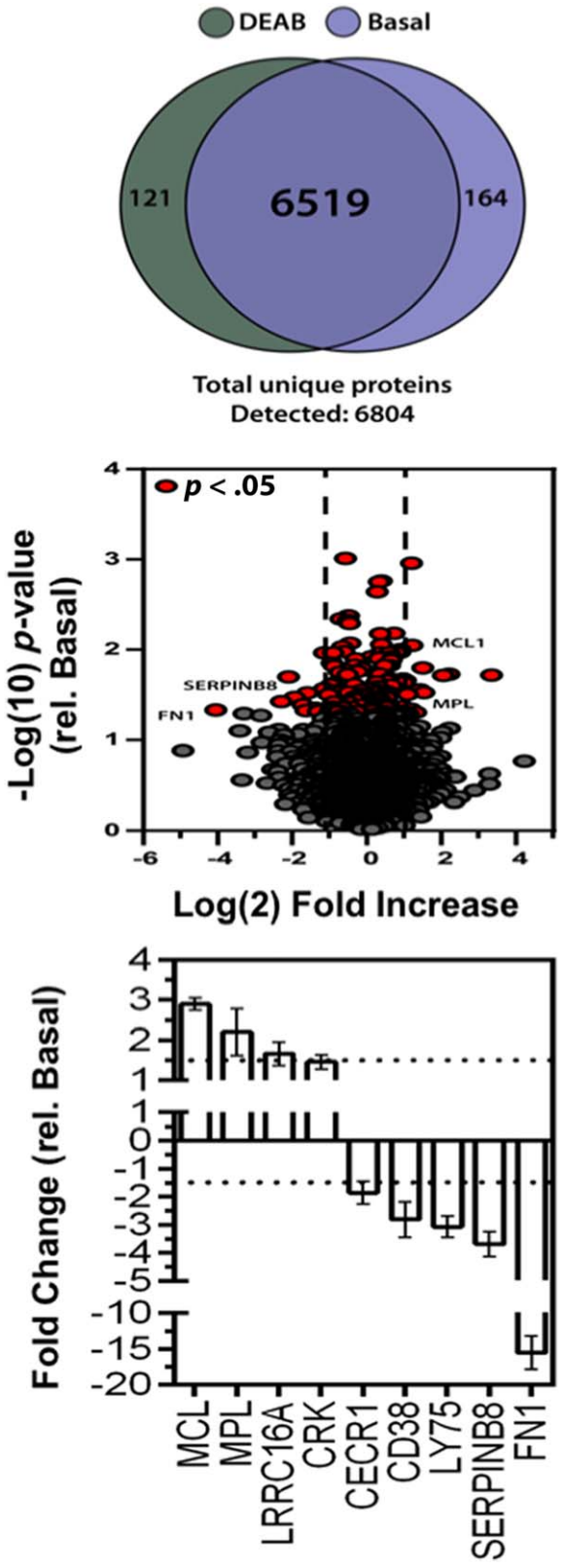

Figure 4.

DEAB-Treated Cells Demonstrated a Pro-Survival and Pro-Angiogenic Proteome

We used highly sensitive mass spectrometry to compare global proteome changes after 9 days expansion under either Basal ($N = 3$) or DEAB-treated ($N = 3$) conditions. Expanded UCB ALDH^{hi} cells generated a heterogeneous cell population comprised of several hematopoietic cell types after 9 days [28]; therefore, detectable changes in the global proteome should reflect changes within influential signaling networks. The proteomic profiles of these expanded cell populations were remarkably similar. Of the 6,804 unique proteins detected, only 121 proteins were unique to cells harvested from DEAB-treated conditions, and 164 were unique to cells harvested from Basal conditions, (Fig. 4A). Proteins exclusively expressed under DEAB-treated conditions were largely associated with anti-apoptotic activity (i.e., NEMO, IKBKG; Caspase Recruitment Domain-containing protein 6, CARD6; Supporting Information Table S4). Conversely, proteins exclusive to Basal conditions included drivers of apoptosis, including Fas cell surface death receptor (FAS) (Supporting Information Table S5). Several proteins implicated with mature hematopoietic cell functions (i.e., plasminogen activator; platelet-activating factor receptor; dendritic cell-associated lectin 2; integrin subunit beta 7) were exclusively produced under Basal conditions.

Of the 6,519 proteins common to cells from Basal and DEAB-treated conditions, only 117 proteins demonstrated a >1.2-fold or <1.2-fold difference comparing DEAB-treated to Basal conditions (Fig. 4B, 4C). Common angiogenic factors (ANGPT1; von Willebrand factor, vWF; and transforming growth factor beta 1) were comparable in the proteome of Basal and DEAB-treated cells. Interestingly, DEAB-treatment primarily upregulated intracellular proteins involved in the prevention of apoptosis (i.e., BCL2 family apoptosis regulator, MCL1), in the preservation of progenitor cell function (thrombopoietin receptor, MPL), or with cell motility such as proto-oncogene C-Crk (CRK) and leucine rich repeat containing 16A. Cells harvested from Basal conditions upregulated proteins primarily associated with HPC differentiation; including Fibronectin (FN1), Serpin family B member 8 (SERPINB8), lymphocyte antigen 75 (LY75), and adenosine deaminase 2 (CECR1). Validating our flow cytometry data, CD38 protein levels were decreased 1.68-fold in cells harvested after DEAB-treatment compared with Basal conditions. Collectively, these analyses suggest that DEAB-treatment increased the production of pro-survival proteins and decreased the production of proteins associated with hematopoietic differentiation.

Figure 4. Distinct proteomic profiles for diethylaminobenzaldehyde (DEAB)-treated versus Basal cells. **(A):** Mass spectrometry identified 6804 individual proteins across cell lysates. Of the 6,519 proteins detected in both Basal and DEAB-treated cells ($N = 3$), only 137 proteins were found to be **(B)** differentially expressed (red circles, *, $p < .05$). **(C):** DEAB-treatment increased production of anti-apoptotic proteins, including myeloid cell leukemia-1 (MCL1) and thrombopoietin receptor (MPL). Decreased detection of differentiation factors including CD38, CECR1, SERPINB8, and Fibronectin (FN1) was also observed in DEAB-treated cells. Statistical analyses were performed by students *t* test. Abbreviation: DEAB, diethylaminobenzaldehyde.

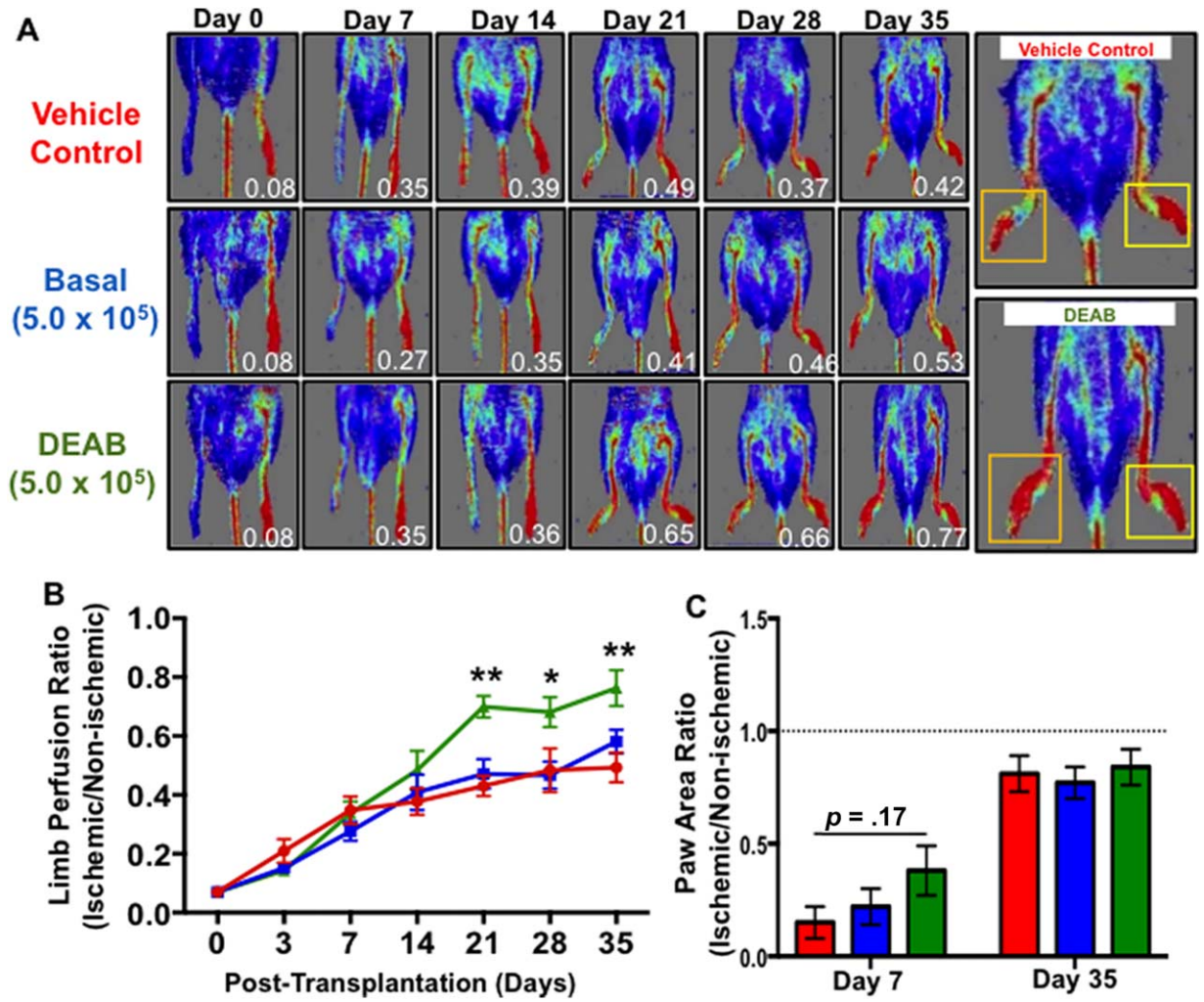

Figure 5. Diethylaminobenzaldehyde (DEAB)-treated cells accelerated the recovery of limb perfusion after transplantation. **(A):** Representative laser Doppler perfusion imaging following femoral artery ligation and intramuscular (i.m.) transplantation of phosphate-buffered saline (PBS) ($n = 7$), 5×10^5 Basal cells ($n = 11$) or 5×10^5 DEAB-treated cells ($n = 11$). Perfusion ratio (PR) in the ischemic (orange box) versus non-ischemic (yellow box) limbs are shown in white text. **(B):** Non-obese diabetic/severe combined immunodeficient mice were i.m. injected with Basal cells showed similar recovery of perfusion compared with PBS controls (day 35 PR $= 0.58 \pm 0.04$ vs. 0.49 ± 0.06; respectively). Transplantation of DEAB-treated cells enhanced the recovery of limb perfusion compared with PBS vehicle controls or Basal cells at days 21–35. **(C):** Paw area ratio of ischemic vs. non-ischemic limb measure at 7 and 35 days post-transplantation ($n = 5$–7). DEAB-treated cells modestly increased limb usage at 7 days post-transplantation, although limb usage was equal across transplantation conditions at day 35 post-transplantation. Data represented as mean ± SEM (*, $p < .05$, **, $p < .01$). Statistical analyses were performed by analysis of variance with Tukey's multiple comparisons test relative to PBS-injected mice. Abbreviation: DEAB, diethylaminobenzaldehyde.

Transplantation of DEAB-Treated Cells Accelerated the Recovery of Perfusion

We have previously shown that extended culture of UCB ALDH^{hi} cells resulted in the loss of vascular regenerative functions after transplantation in vivo [28]. Therefore, we sought to determine whether DEAB-treatment could generate cells that retained vascular regenerative function following transplantation into mice with hind-limb ischemia. After unilateral FAL surgery, non-obese diabetic/severe combined immunodeficient (*NOD/SCID*) mice with hind-limb ischemia (Perfusion Ratio, PR; PR < 0.1) received i.m. injection of UCB ALDH^{hi} cells expanded for 9 days under Basal or DEAB-treated culture conditions. Transplantation of 5.0×10^5 cells generated under Basal conditions failed to improve limb perfusion from baseline recovery observed with PBS-injected controls (PR $= 0.58 \pm 0.04$ vs. 0.49 ± 0.05 at day 35, respectively; Fig. 5A, 5B). However, i.m.-transplantation with 5.0×10^5 cells generated under DEAB-treated conditions significantly increased limb perfusion as early as day 21, compared with PBS controls (0.70 ± 0.04 vs. 0.43 ± 0.03; **, $p < .01$), and improved limb perfusion persisted until day 35 post-transplantation (0.76 ± 0.06; **, $p < .01$). Limb usage assessed by Catwalk paw print area measurements for all groups were equivalent at day 35. However, at 7 days post-transplantation mice that received DEAB-treated cells showed modestly improved limb usage compared with PBS-controls ($p = .17$).

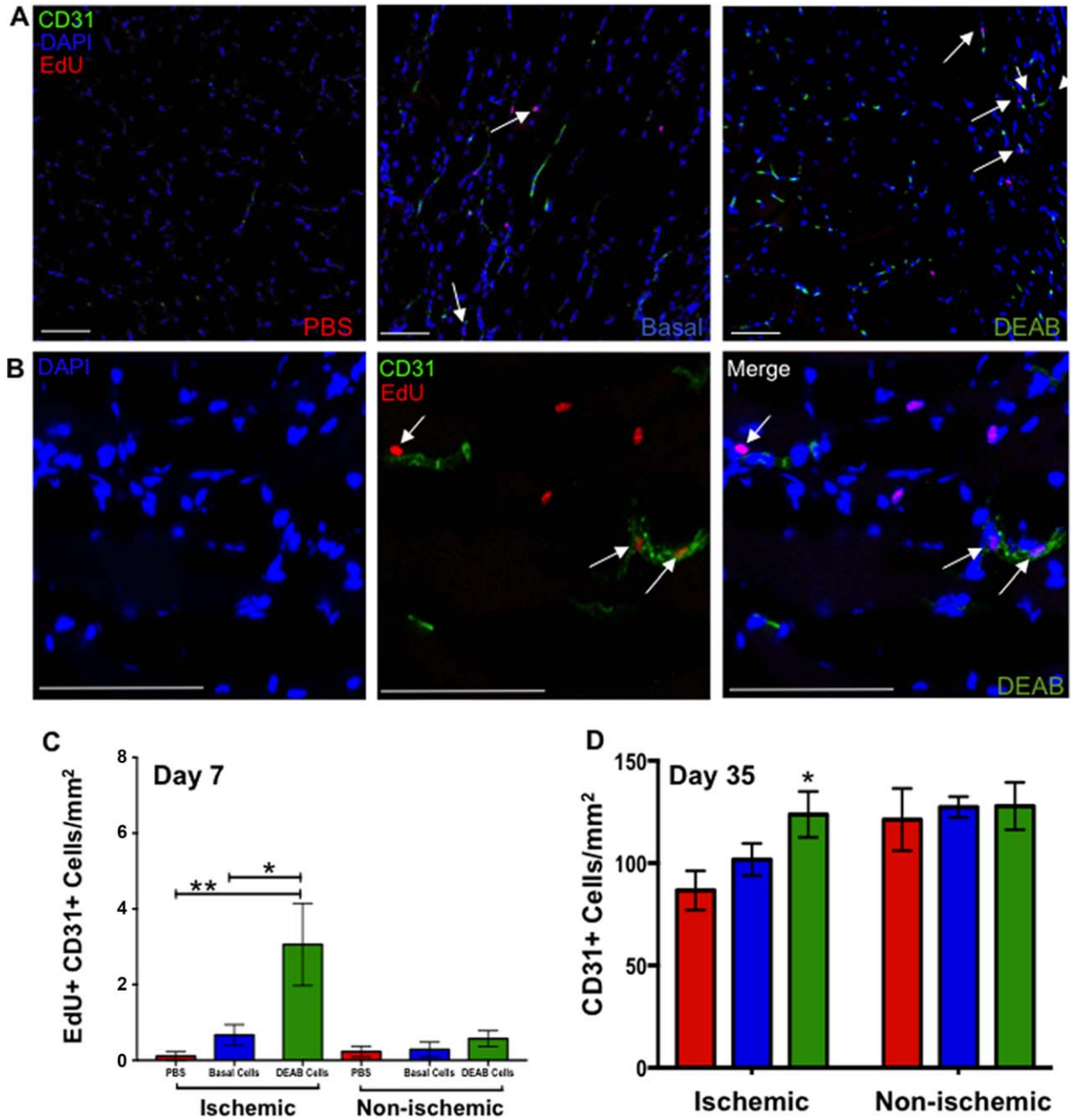

Figure 6. Transplantation of diethylaminobenzaldehyde (DEAB)-treated cells increased capillary density via increasing murine endothelial cell proliferation. Non-obese diabetic/severe combined immunodeficient mice transplanted with either phosphate-buffered saline (PBS) ($n = 5$), Basal cells ($n = 6$), or DEAB-treated cells ($n = 6$) were injected with EdU 24 hours before euthanasia at 7 days post-transplantation. **(A):** Representative confocal images (×10) of cryosectioned thigh muscles stained for endothelial cell marker (CD31) and EdU-incorporation (Alexafluor 594).**(B):** Representative confocal image (×40) of endothelial cell proliferation (EdU+/CD31+) in the ischemic limb of mice transplanted with DEAB-treated cells. **(C):** Mice transplanted with DEAB-treated cells had a significantly increased number of proliferating endothelial cells within the ischemic limb, compared with PBS-injected or Basal cell transplanted mice. **(D):** Intramuscular transplantation of DEAB-treated cells increased CD31+ capillary density in ischemic limbs of mice killed at day 35 ($n = 7$–11). Data represented as mean ± SEM.(*, $p < .05$; **, $p < .01$). Statistical analyses were performed by analysis of variance with Tukey's multiple comparisons test. Scale bar = 150 μm. Abbreviations: DAPI, 4′,6-diamidino-2-phenylindole; DEAB, diethylaminobenzaldehyde; PBS, phosphate-buffered saline.

Transplantation of DEAB-Treated Cells Stimulated Endothelial Cell Proliferation and Increased Capillary Density within Ischemic Limbs

To investigate potential mechanisms by which DEAB-treated cells accelerated the recovery of limb perfusion, vascular density was assessed alongside human cell engraftment kinetics at day 7 and day 35 post-transplantation in ischemic thigh muscle tissue sections. Human cell engraftment was detected within ischemic thigh muscles at 7-days post-transplantation with either Basal or DEAB-treated cells (Supporting Information Fig. S3). Compared with Basal cells, DEAB-treated cells demonstrated a trend toward increased engraftment within

the ischemia thigh muscle (1.25 ± 0.21 vs. 0.83 ± 0.11 HLA+ cells/mm^2, $n = 4$, $p = .13$). Moreover, transplanted cells were not detected after 35-days post-transplantation. Mice were injected with EdU 24 hours before euthanasia to allow quantification of proliferating CD31+ endothelial cells. At day 7 post-transplantation, mice transplanted with DEAB-treated cells showed an increased number of EdU+/CD31+ cells/mm^2 within ischemic thigh muscle, compared with mice injected with cells generated under Basal conditions (3.06 ± 1.08 vs. 0.67 ± 0.27, *, $p < .05$) or PBS (0.11 ± 0.11, **, $p < .01$; Fig. 6A, 6B). Augmented endothelial cell proliferation corresponded to increased CD31+ capillary density at day 35 with DEAB-treated cells (*, $p < .05$; Fig. 6C). In addition, mice transplanted with DEAB-treated cells increased the number of larger vessels expressing vWF at day 35 (Supporting Information Fig. 4), compared with PBS-injected controls. Collectively, DEAB-treated cells survived for at least 7 days post-transplantation and stimulated endothelial cell proliferation leading to increased vascular density in the ischemic limb.

Discussion

Blood-derived progenitor cells with ALDH^{hi}-activity demonstrate multifaceted regenerative functions in preclinical studies [12, 15]. However, it is becoming well accepted in preclinical studies that harvesting autologous cells from the BM of individuals with diffuse atherosclerosis [19] and associated comorbidities such as obesity and type 2 diabetes [20, 37], results in the accrual of progenitor cells with depleted numbers and dysfunctional vascular regenerative capacity. The use of allogenic UCB cells with limited exposure to damaging metabolic by-products of chronic disease [24] may mitigate progenitor cell exhaustion and facilitate the development of cellular therapies with improved efficacy. UCB represents a readily accessible source of regenerative cells, usually considered discarded material, and is easily harvested with no risk to either the newborn or mother. Recent establishment of national cord blood banking programs generates a renewable multidonor pool with increased diversity for HLA-matching and subsequent use in allogeneic therapeutic applications. A phase I clinical trial (NCT01019681) was recently initiated to determine the safety and efficacy of UCB-MNC; however, these results have yet to be reported. We have previously demonstrated enhanced vascular regenerative functions of UCB-derived ALDH^{hi} cells compared with unpurified UCB-MNC [12]. However, ALDH^{hi} cells only represent <0.5% of total UCB-MNC and require ex vivo expansion to increase the number of progenitor cells needed to support early preclinical studies. Herein, we demonstrate an expansion strategy and early preclinical evidence which indicates expanded allogeneic UCB ALDH^{hi} cells could be used for treating severe ischemic disease [16].

UCB ALDH^{hi} cells are primarily comprised of early myeloid HPC [12] that can be efficiently expanded in short-term culture under serum-free conditions [28]. Unfortunately, when culture time was extended from 6 to 9 days, the vascular regenerative function of expanded progeny was diminished after i.m.-transplantation into *NOD/SCID* mice with hind-limb ischemia [23]. This led us to speculate that prolonged culture time under serum-free (Basal) conditions reduced pro-angiogenic growth factor production and/or secretion, such as VEGF-A, from expanded progeny. Despite robust differentiation toward the megakaryocyte lineage between days 6 and 9, we did not observe significant decrease in secreted levels of common pro-angiogenic growth factors (VEGF-A, ANGPT1, CCL5). In contrast, we observed an increased expression of megakaryocyte lineage-specific proteins, including CD41 (ITGA2B) and CD42 (GPIB). Specifically, flow cytometry analyses demonstrated a reduction of primitive surface marker (CD34) expression alongside diminished ALDH-activity, which coincided with the acquisition of a mature megakaryocyte phenotype (CD41+/CD42+/CD38+).

Megakaryocytes represent large hematopoietic cells (50–100 μm) which release platelets into systemic circulation through the fragmentation of proplatelet extensions that protrude into vascular sinuses of the BM niche. The turnover of circulating platelets is frequent (<9 days); therefore, the consistent production of platelets is necessary to ensure vessel hemostasis and injury repair [38, 39]. Platelet-derived CD42 binds to vWF on exposed subendothelium collagen during vascular injury, the subsequent activation of platelets will stimulate soluble protein and extracellular vesicle secretion into the local microenvironment and systemic circulation. These stimuli recruit and activate biological processes within endothelial or hematopoietic cells [38, 40, 41]. Specifically, platelet-derived stimuli (i.e., VEGF-A) influence both angiogenic and inflammatory pathways during wound healing and vascular regeneration in vitro and in vivo [39, 40, 42]. To our knowledge, this is the first study to characterize and investigate the vascular regenerative potential of a culture-expanded, megakaryocyte-enriched cell population for treating ischemic disease. Indeed, the acquisition of a mature megakaryocyte phenotype (CD41+/CD42+/CD38+) and concomitant loss of ALDH^{hi}-activity under Basal conditions diminished the vascular regenerative capacity of UCB-derived ALDH^{hi} cells.

Chute et al. were the first to show that DEAB-treatment enhanced the expansion of UCB-derived CD34 + CD38$^-$ cells with SCID repopulating capacity. Specifically, DEAB-treated cultures were enriched 11.6-fold with cells retaining primitive CD34+/CD38$^-$ phenotype after 7 days. The benefit of DEAB-treatment was reversed after RA-supplementation, suggesting that inhibition of ALDH-activity promoted HSC self-renewal via reduced RA-production. Our study extends these findings to show that inhibition of ALDH-activity and RAR/RXR complex activation could modify the transcription of downstream targets (i.e., CYP26A1) [29]. Despite equal expansion of CD34+ cells compared with Basal conditions, DEAB-treated progeny better retained a primitive phenotype, with a 15-fold expansion in CD34 + CD38$^-$ cells and an 11-fold expansion of the most primitive ALDH^{hi}/CD34+/CD38$^-$ cells. Importantly, DEAB-treatment significantly increased multipotent myeloid colony formation in vitro, suggesting that ALDH^{hi} activity can segregate multipotent CD34+ cells from committed, unipotent ALDH^{lo} CD34+ cells [43].

Under Basal conditions, rapid loss of ALDH^{hi}-activity coincided with the acquisition of mature hematopoietic surface marker, CD38. In contrast, DEAB-treatment enhanced retention of ALDH^{hi} phenotype and reduced CD38 expression. CD38 (Cyclic Ribose ADP Hydrolase) is a multifunctional enzyme implicated with intracellular Ca+ signaling, platelet

aggregation, and adhesion of leukocytes to CD31+ endothelial cells [44, 45]. CD38 is also a direct target of RA-signaling [27], suggesting that DEAB-treatment limited CD38 expression by modifying RA-signaling networks. Furthermore, DEAB-treated cell lysates exhibited increased levels of MCL1 and MPL, cellular proteins implicated with progenitor cell maintenance [46, 47]. Conversely, Basal conditions, increased the expression of proteins implicated with hematopoietic differentiation (i.e., CECR1, FN1, SERPINB8, and LY75). Collectively, flow cytometry and proteomic data confirmed DEAB-treatment enhanced the expansion of multipotent HPC by limiting RA-induced differentiation.

We next investigated whether differentiation toward the megakaryocyte lineage was delayed by the inhibition of RA-production. Commitment to the megakaryocyte lineage is marked by the acquisition of CD41 (ITGA2B), whereas CD42 (GP1B) expression occurs later in megakaryopoiesis [48]. However, acquisition of CD41 and CD42 expression was not altered by DEAB-treatment. This was not a surprise considering treatment with TPO and FLT-3L is known to drive early megakaryopoiesis and increase CD41 expression during ex vivo expansion [49]. Several reports have suggested that cells with the immature megakaryoblast phenotype ($CD34+/CD38^{-}/CD41+/CD42^{-}$) retain multipotentcy in vitro and in vivo [36, 50, 51]. DEAB-treatment increased the accumulation of $CD34+/CD38^{-}$ progenitor cells and delayed the acquisition of CD38 within the megakaryoblast lineage ($CD41+/CD42^{-}$). DEAB-treatment also limited the production of mature megakaryocytes (CD41+/CD42+/CD38+); suggesting that inhibition of RA-production delayed differentiation at multiple stages of megakaryopoeisis.

Although the secretome and proteome of day 9 Basal cells showed similar expression of pro-angiogenic stimuli (i.e., VEGF-A), day 9 Basal cells did not support the recovery of perfusion after i.m. transplantation into the ischemic limb of *NOD*/*SCID* mice. In contrast, DEAB-treated cells accelerated the recovery of blood perfusion by increasing endothelial cell proliferation in ischemic muscle tissue. Both Basal and DEAB-treated cells were detected 7-days post-transplantation, but were absent at day 35. DEAB-treated cells demonstrated a trend toward increased engraftment and were found to be closely associated with proliferating endothelial cells, however, did not engraft into murine vasculature. Thus, we predict that survival and/or migration to a regenerative niche is compromised in day 9 Basal cells following i.m.-transplantation. In support of this interpretation, day 9 Basal cells exclusively expressed proteins implicated with the induction of apoptosis, including FAS [52]. In contrast, DEAB-treated cells exclusively expressed several pro-survival molecules (i.e., CARD6, MCL1, KRT18, etc.), in addition to retaining the cytoprotective functions of $ALDH^{hi}$-activity. Further studies are warranted to determine the role of apoptotic and pro-survival pathways identified in this study. Several studies have demonstrated increased regenerative cell function by pre-treating cells with small molecules to enhance survival following transplantation [53, 54]. Our data suggest DEAB-treatment generated heterogeneous myeloid cell progeny with pro-angiogenic secretory capacity that were more likely to survive i.m.-transplantation into a harsh ischemic microenvironment. Furthermore, our data suggest $ALDH^{hi}$ -activity and reduced CD38 expression may be a characteristic of vascular regenerative hematopoietic cells. Especially considering day 9 DEAB-treated, day 6 Basal, and fresh UCB $ALDH^{hi}$ cells [12] share these characteristics ($ALDH^{hi}/CD38^{lo}$), in contrast to day 9 Basal cells with diminished vascular regenerative functions ($ALDH^{lo}/CD38^{hi}$).

Both Basal and DEAB-treated cells were identified by proteomics to equally express integrin complexes including CD41,CD61, CD18, and CD29 after culture on fibronectin. Activation of integrin signaling is expected to increase transplanted cells survival and/or migration. In contrast, detachment induced apoptosis could negatively impact transplanted cell engraftment. In addition, UCB $ALDH^{hi}$ cells cultured under Basal conditions for 9 days increased the production of extracellular matrix (ECM) molecules (fibronectin and collagen), compared with DEAB-treated cells. The increased production of ECM molecules is characteristic of cells within the megakaryocyte lineage that could potentially limit bio-distribution throughout the ischemic muscle. Additional studies are needed to specifically address whether pre-exposure to a matrix influences the engraftment and bio-distribution of transplanted progenitor cells. Interestingly, Whiteley et al. demonstrated UCB-derived CD34+/CD45+ cells cultured for 8 days, engrafted ischemic murine muscle tissue at a higher rate than uncultured CD34+ cells or MNC, suggesting that ex vivo culture may benefit cellular therapies for PAD [55]. Several early trials have reported modest clinical benefits following the i.m. transplantation of expanded progenitor cells from autologous BM or peripheral blood [56, 57]; however, these trials were unable to improve limb amputation rates.

In summary, our previous studies established that UCB $ALDH^{hi}$ cells and day 6 expanded progeny temporally engraft ischemic muscle tissues and induce neovascularization in *NOD*/*SCID* mice with hind-limb ischemia [28]. Unfortunately, the low number of transplantable cells would limit or impede a controlled clinical study to effectively investigate currently unestablished parameters of expandable UCB-cells, such as clinical efficacy and cell dose. This study demonstrates limiting RA-induced differentiation during UCB-cell expansion can expand total cell number by ~80-fold, and total $ALDH^{hi}$ cells by ~25-fold, without a significant loss of vascular regenerative function. Therefore, we consider these results early preclinical evidence that reasonable cell numbers can be generated from a single UCB sample to assess currently undetermined parameters leading to improved efficacy, such as cell dose, phenotype (ALDH, CD34, CD38, etc.), or therapeutic cell source (BM vs. UCB). Collectively, (a) advanced understanding of signaling pathways which drive progenitor cell differentiation, (b) identification of vascular regenerative cell subpopulations, and (c) improving culture conditions to facilitate cell type specific expansion is warranted for the development of effective vascular regenerative therapies.

Acknowledgments

We thank Kristin Chadwick at the London Regional Flow Cytometry Facility for cell sorting. This work was supported by an operating grant from the Canadian Institute of Health Research (CIHR) (MOP# 378189) and a grant-in-aid from the Heart and Stroke Foundation of Canada (GIA/13/0001612).

Author Contributions

T.T.C.: conception and design, collection and/or assembly of data, data analysis and interpretation, manuscript writing; S.E.S. and M.K.: collection and/or assembly of data, data analysis and interpretation; G.I.B.: collection and/or assembly of data; G.A.L: provision of study material, final approval of manuscript; D.A.H: conception and design, financial support, collection and/or assembly of data, data analysis and interpretation, manuscript writing, final approval of manuscript.

Disclosure of Potential Conflicts of Interest

The authors indicated no potential conflicts of interest.

References

1 Sowers JR, Stump CS. Insights into the biology of diabetic vascular disease: What's new? Am J Hypertens 2004;17:2S–6S.
2 Golomb BA, Dang TT, Criqui MH. Peripheral arterial disease. Circulation 2006;114:688–699.
3 Vartanian SM, Conte MS. Surgical intervention for peripheral arterial disease. Circ Res 2015;116:1614–1628.
4 Makowsky M, McMurtry MS, Elton T et al. Prevalence and treatment patterns of lower extremity peripheral arterial disease among patients at risk in ambulatory health settings. Canadian J Cardiol 2011;27:389. e11–389. e18.
5 Bonaca MP, Creager MA. Pharmacological treatment and current management of peripheral artery disease. Circ Res 2015;116:1579–1598.
6 Thukkani AK, Kinlay S. Endovascular intervention for peripheral artery disease. Circ Res 2015;116:1599–1613.
7 Criqui MH, Aboyans V. Epidemiology of peripheral artery disease. Circ Res 2015;116:1509–1526.
8 Davies MG. Criticial limb ischemia: Epidemiology. Method DeBakey Cardiovasc J 2012;8:10–14.
9 Wahlberg E. Angiogenesis and arteriogenesis in limb ischemia. J Vasc Surg 2003;38:198–203.
10 Arpino J-M, Nong Z, Li F et al. 4D Microvascular analysis reveals that regenerative angiogenesis in ischemic muscle produces a flawed microcirculation. Circ Res 2017;120:1453–1465.
11 Lawall H, Bramlage P, Amann B. Stem cell and progenitor cell therapy in peripheral artery disease. Thromb Haemost 2010;103:696–709.
12 Putman DM, Liu KY, Broughton HC et al. Umbilical cord blood-derived aldehyde dehydrogenase-expressing progenitor cells promote recovery from acute ischemic injury. Stem Cells 2012;30:2248–2260.
13 Capoccia BJ, Robson DL, Levac KD et al. Revascularization of ischemic limbs after transplantation of human bone marrow cells with high aldehyde dehydrogenase activity. Blood 2009;113:5340–5351.
14 Bell GI, Meschino MT, Hughes-Large JM et al. Combinatorial human progenitor cell transplantation optimizes islet regeneration through secretion of paracrine factors. Stem Cells Dev 2012;21:1863–1876.
15 Seneviratne AK, Bell GI, Sherman SE et al. Expanded hematopoietic progenitor cells reselected for high aldehyde dehydrogenase activity demonstrate islet regenerative functions. Stem Cells 2016;34:873–887.
16 Perin EC, Silva G, Gahremanpour A et al. A randomized, controlled study of autologous therapy with bone marrow–derived aldehyde dehydrogenase bright cells in patients with critical limb ischemia. Catheteriz Cardiovasc Interv 2011;78:1060–1067.
17 Perin EC, Murphy M, Cooke JP et al. Rationale and design for PACE: Patients with intermittent claudication injected with ALDH bright cells. Am Heart J 2014;168:667–673. e2.
18 Perin EC, Murphy MP, March KL et al. Evaluation of cell therapy on exercise performance and limb perfusion in peripheral artery disease. Circulation 2017;135:1417–1428.
19 Heeschen C, Lehmann R, Honold J et al. Profoundly reduced neovascularization capacity of bone marrow mononuclear cells derived from patients with chronic ischemic heart disease. Circulation 2004;109:1615–1622.
20 Fadini GP, Sartore S, Albiero M et al. Number and function of endothelial progenitor cells as a marker of severity for diabetic vasculopathy. Arterioscl Thromb Vasc Biol 2006;26:2140–2146.
21 Tan Q, Qiu L, Li G et al. Transplantation of healthy but not diabetic outgrowth endothelial cells could rescue ischemic myocardium in diabetic rabbits. Scand J Clin Lab Invest 2010;70:313–321.
22 Losordo DW, Kibbe MR, Mendelsohn F et al. A randomized, controlled pilot study of autologous CD34+ cell therapy for critical limb ischemia. Circulation 2012;5:821–830.
23 Giugliano D, Ceriello A, Paolisso G. Oxidative stress and diabetic vascular complications. Diabetes Care 1996;19:257–267.
24 Brownlee M. Biochemistry and molecular cell biology of diabetic complications. Nature 2001;414:813–820.
25 Rhinn M, Dollé P. Retinoic acid signalling during development. Development 2012;139:843–858.
26 Gudas LJ. Retinoids induce stem cell differentiation via epigenetic changes. Semin Cell Dev Biol 2013;24:701. 10.1016/j.semcdb.2013.08.002.
27 Drach J, McQueen T, Engel H et al. Retinoic acid-induced expression of CD38 antigen in myeloid cells is mediated through retinoic acid receptor-α. Cancer Res 1994;54:1746–1752.
28 Putman DM, Cooper TT, Sherman SE et al. Expansion of umbilical cord blood aldehyde dehydrogenase expressing cells generates myeloid progenitor cells that stimulate limb revascularization. Stem Cells Translational Medicine 2017;6:1607–1619.
29 Chute JP, Muramoto GG, Whitesides J et al. Inhibition of aldehyde dehydrogenase and retinoid signaling induces the expansion of human hematopoietic stem cells. Proc Natl Acad Sci USA 2006;103:11707–11712.
30 Ghiaur G, Yegnasubramanian S, Perkins B et al. Regulation of human hematopoietic stem cell self-renewal by the microenvironment's control of retinoic acid signaling. Proc Natl Acad Sci USA 2013;110:16121–16126.
31 Wessel D, Flügge U. A method for the quantitative recovery of protein in dilute solution in the presence of detergents and lipids. Anal Biochem 1984;138:141–143.
32 Kulak NA, Pichler G, Paron I et al. Minimal, encapsulated proteomic-sample processing applied to copy-number estimation in eukaryotic cells. Nat Methods 2014;11:319–324.
33 Cox J, Mann M. MaxQuant enables high peptide identification rates, individualized ppb-range mass accuracies and proteome-wide protein quantification. Nat Biotechnol 2008;26:1367–1372.
34 Cox J, Hein MY, Luber CA et al. Accurate proteome-wide label-free quantification by delayed normalization and maximal peptide ratio extraction, termed MaxLFQ. Mol Cell Proteom 2014;13:2513–2526.
35 Tyanova S, Temu T, Sinitcyn P et al. The Perseus computational platform for comprehensive analysis of (prote) omics data. Nat Methods 2016;13:731–740.
36 Debili N, Robin C, Schiavon V et al. Different expression of CD41 on human lymphoid and myeloid progenitors from adults and neonates. Blood 2001;97:2023–2030.
37 Hess DA, Hegele RA. Linking diabetes with oxidative stress, adipokines, and impaired endothelial precursor cell function. Canadian J Cardiol 2012;28:629–630.
38 Italiano JE, Richardson JL, Patel-Hett S et al. Angiogenesis is regulated by a novel mechanism: Pro-and antiangiogenic proteins are organized into separate platelet α granules and differentially released. Blood 2008;111:1227–1233.
39 Brill A, Dashevsky O, Rivo J et al. Platelet-derived microparticles induce angiogenesis and stimulate post-ischemic revascularization. Cardiovasc Res 2005;67:30–38.
40 Barry OP, Praticò D, Lawson JA et al. Transcellular activation of platelets and endothelial cells by bioactive lipids in platelet microparticles. J Clin Invest 1997;99:2118.
41 Chatterjee M, Gawaz M. Platelet-derived CXCL12 (SDF-1α): Basic mechanisms and clinical implications. J Thromb Haemost 2013;11:1954–1967.
42 Kim HK, Song KS, Chung JH et al. Platelet microparticles induce angiogenesis in vitro. Br J Haematol 2004;124:376–384.
43 Storms RW, Green PD, Safford KM et al. Distinct hematopoietic progenitor compartments

are delineated by the expression of aldehyde dehydrogenase and CD34. Blood 2005;106:95–102.
44 Mushtaq M, Nam T-S, Kim U-H. Critical role for CD38-mediated Ca2+ signaling in thrombin-induced procoagulant activity of mouse platelets and hemostasis. J Biol Chem 2011;286:12952–12958.
45 Deaglio S, Morra M, Mallone R et al. Human CD38 (ADP-ribosyl cyclase) is a counter-receptor of CD31, an Ig superfamily member. J Immunol 1998;160:395–402.
46 Campbell CJ, Lee JB, Levadoux-Martin M et al. The human stem cell hierarchy is defined by a functional dependence on Mcl-1 for self-renewal capacity. Blood 2010;116:1433–1442.
47 Yoshihara H, Arai F, Hosokawa K et al. Thrombopoietin/MPL signaling regulates hematopoietic stem cell quiescence and interaction with the osteoblastic niche. Cell Stem Cell 2007;1:685–697.
48 Klimchenko O, Mori M, DiStefano A et al. A common bipotent progenitor generates the erythroid and megakaryocyte lineages in embryonic stem cell–derived primitive hematopoiesis. Blood 2009;114:1506–1517.
49 Li K, Yang M, Lam AC et al. Effects of flt-3 ligand in combination with TPO on the expansion of megakaryocytic progenitors. Cell Transplant 2000;9:125–131.
50 Gekas C, Graf T. CD41 expression marks myeloid-biased adult hematopoietic stem cells and increases with age. Blood 2013;121:4463–4472.
51 Basch RS, Zhang XM, Dolzhanskiy A et al. Expression of CD41 and c-mpl does not indicate commitment to the megakaryocyte lineage during haemopoietic development. Br J Haematol 1999;105:1044–1054.
52 Hirata H, Takahashi A, Kobayashi S et al. Caspases are activated in a branched protease cascade and control distinct downstream processes in Fas-induced apoptosis. J Exp Med 1998;187:587–600.
53 Seeger FH, Zeiher AM, Dimmeler S. Cell-enhancement strategies for the treatment of ischemic heart disease. Nat Clin Pract Cardiovasc Med 2007;4:S110–S113.
54 Chavakis E, Urbich C, Dimmeler S. Homing and engraftment of progenitor cells: A prerequisite for cell therapy. J Mol Cell Cardiol 2008;45:514–522.
55 Whiteley J, Bielecki R, Li M et al. An expanded population of CD34+ cells from frozen banked umbilical cord blood demonstrate tissue repair mechanisms of mesenchymal stromal cells and circulating angiogenic cells in an ischemic hind limb model. Stem Cell Rev Rep 2014;10:338–350.
56 Powell RJ, Marston WA, Berceli SA et al. Cellular therapy with Ixmyelocel-T to treat critical limb ischemia: The randomized, double-blind, placebo-controlled RESTORE-CLI trial. Mol Ther 2012;20:1280–1286.
57 Szabó GV, Kövesd Z, Cserepes J et al. Peripheral blood-derived autologous stem cell therapy for the treatment of patients with late-stage peripheral artery disease—Results of the short-and long-term follow-up. Cytotherapy 2013;15:1245–1252.


See www.StemCells.com for supporting information available online.